HITRAN 2012 refractive indices ☆

S.T. Massie [a],[*], M. Hervig [b]

[a] National Center for Atmospheric Research, Boulder, CO 80307, USA
[b] GATS Inc., PO Box 449, Driggs, ID 83422, USA

ARTICLE INFO

ABSTRACT

The HITRAN 2012 compilation of the real and imaginary refractive indices of the materials in aerosols and cloud particles is reviewed. Additions to HITRAN 2012 focus upon materials that are absorptive (i.e. minerals, burning vegetation, brown carbon, desert dust, and volcanic ash). The HITRAN-RI program, created to facilitate usage of the indices, is discussed. The HITRAN-RI program inter-compares the indices of different data sets and calculates optical properties (i.e. extinction, scattering, absorption, single scattering albedo, backscattering, and asymmetry parameter) for user specified size distributions and particle types. The instructional component of HITRAN-RI introduces the user to Mie calculations for spheres and coated spheres, and applies various mixing rules by which one calculates the effective indices of a multi-component particle.

1. Introduction

Liquid and solid particles exert influence in the atmosphere by scattering and absorbing light [1,2], by acting as nuclei in the cloud formation processes [3], and by taking part in chemical reactions in the troposphere and stratosphere [4,5]. The physics and wavelength dependence of light scattering is dependent upon particle size, shape, and composition [6,7]. Refractive indices of different materials are used in light scattering calculations to account for the compositional characteristics of particles. Since there is a wide range of particle types, sizes, shapes, and compositions, distributed in the atmosphere in a complicated spatial and temporal manner, liquid and solid particles complicate our ability to accurately quantify radiative transfer in the Earth's atmosphere.

Particles also are of importance because they complicate the interpretation of remote sensing experiments. Volcanic eruptions, such as Mt. Pinatubo in 1991, injected large amounts of SO_2 into the stratosphere, which resulted in data gaps in solar occultation measurement due to the very large optical depths of the ensuing stratospheric sulfate aerosol. The future Orbiting Carbon Observatory (OCO-2) experiment will measure CO_2 on a global basis [8]. The retrieval of the CO_2 column, however, is impacted by the presence of aerosols and prohibited if opaque clouds are present. The future Pre-Aerosol Clouds and Ecosystem (PACE) experiment will measure ocean color (e.g. phytoplankton concentrations) on a global basis at high spectral resolution [9]. Uncertainties in the types of aerosol(s) that scatter and absorb light will impact the retrieval accuracy of chlorophyll concentrations. As it becomes more difficult for experiments to achieve their primary measurement goals, the need to account accurately for the effects of liquid and solid particles upon radiative transfer becomes more acute.

In this paper we describe the refractive indices included in the 2012 HIgh-resolution TRANsmission (HITRAN) compilation [10], and describe a new computer program associated with this compilation, called HITRAN-Refractive

---

* Corresponding author.
E-mail addresses: massie@ucar.edu (S.T. Massie),
m.e.hervig@gats-inc.com (M. Hervig).

Indices (HITRAN-RI), which reads in and uses the HITRAN indices in a variety of applications. Associated subdirectories and software associated with HITRAN-RI enables users to apply the HITRAN indices in realistic light scattering calculations, and provides a convenient repository of the original reference papers. HITRAN 2012 indices differ from previous HITRAN [11–13] and Gestion et Etude des Informations Spectroscopiques Atmosphériques (GEISA) [14] tabulations in that there are additional refractive indices, especially for absorptive aerosol, the data are now contained in two different file formats (ascii and netCDF), the original papers of the indices are directly available to the user, and the user can use the (HITRAN-RI) program to apply the indices in applications in a Fortran-90 or Interactive Data Language (IDL) setting.

The HITRAN-RI program has features similar to those incorporated in the Optical Properties of Aerosols and Clouds (OPAC) computer program [15], and additional features. OPAC is based upon laboratory measured indices, and provides optical properties of typical cases of water, ice, and aerosols in the visible and infrared, from 0.25 to 40 μm, and for user-specified mixtures of the various material components. The HITRAN-RI program allows one to inter-compare various indices of the same material type and calculate optical properties for user specified size distributions and particle types. Refractive indices, particle size distributions, and optical properties (i.e. extinction, scattering, absorption, single scattering albedo, backscattering, and asymmetry parameter) are written by the program to output files for external applications. Refractive indices in HITRAN 2012 include those derived from field measurements of aerosols in addition to laboratory measurements of specific compounds. HITRAN-RI also has an instructional component that allows one to become familiar with Mie calculations (for spheres) and coated spheres, and become familiar with various mixing rules by which one calculates the effective indices of a multi-component particle.

This paper is organized as follows. Section 2 describes the indices in HITRAN 2012. Section 3 discusses the features of HITRAN-RI, while Section 4 discusses future developments.

2. 2012 HITRAN refractive indices

The "Aerosols" folder in HITRAN 2012 is comprised of subdirectories: ascii (the ascii files of the indices), netcdf (the netCDF files of the indices), papers (the original journal articles), idl_calc (the IDL version of the HITRAN-RI program), fortran (the Fortran-90 version of the HITRAN-RI program), and archive (contains older data sets). The Aerosols_Readme.pdf gives instructions on how to use the HITRAN-RI program, and the commentary.pdf provides useful information on light scattering references and size distributions. The refractive indices in previous HITRAN compilations [11–13] are included in HITRAN 2012, which contains new datasets (especially for absorptive aerosol). The Aerosols folder and associated subdirectories are available at the HITRAN Database homepage http://www.cfa.harvard.edu/hitran/welcometop.html.

The ASCII file format was the only file format used in previous HITRAN compilations. It is now appropriate to update the listing by storing the data in both ASCII and netCDF files. While the molecular line listings in HITRAN are uniform in the specification of line parameters (i.e. a similar wavenumber, lower state energy level, and pressure broadening coefficient listing format applies to all molecules), the refractive indices are tabulated for a variety of temperatures, weight percent compositions, etc. This non-uniformity makes the ASCII files non-uniform in format structure. The netCDF format serves as a compact way to store the data, since the data from multiple ASCII files for a particular material (e.g. ice at different temperatures as measured by a specific laboratory) are included in a single netCDF file.

The HITRAN compilation contains files of refractive indices measured recently and also data measured decades ago. It is recognized that the accurate specification of multi-decadal multi-satellite measurements is dependent upon knowing the details of the spectroscopy that was used to retrieve molecular species mixing ratios and aerosol parameters. Different experiments have used different spectroscopic aerosol refractive indices and molecular line parameters. This can introduce non-uniform jumps in the time series of a chemical species. NASA satellite programs now require full post-mission documentation of instrument and retrieval details. For these reasons, the HITRAN-RI suite contains new and older refractive indices. One can use HITRAN-RI to determine how the extinction spectrum changes due to variations (and therefore, the uncertainties) in the input refractive index data files.

Refractive indices from the widely used 1985 AFCRL compilation [16] contain several composite data specifications. For example, the "carbonaceous indices" are an average of the indices of a variety of coals [17]. The HITRAN-RI suite contains a "papers" subdirectory which has pdfs of the original papers for all of the refractive index data in HITRAN 2012, plus other pertinent papers. The user can examine e.g. Fig. 1 of Ref. [17] which shows the variations of the imaginary indices from which the composite carbonaceous indices were estimated.

There are admittedly differences between the aggregate refractive indices of aerosols in the real world and the refractive indices of the fundamental materials in HITRAN. While remote sensing in the stratosphere decades ago encountered the effects of particles of a definitive composition (e.g. sulfate aerosols are binary H_2SO_4/H_2O liquid droplets), and models of visibility focused upon light attenuation by water cloud droplets, recent interest in tropospheric chemistry deals with a very complex compositional mix of compounds. Sulfates, ammonium, nitrates, crustal minerals, organic material, and biological material [18] produce a very complex compositional situation. More than 40 trace elements occur in atmospheric particulate matter [5]. Dubovik et al. [19] discusses the considerable ranges in optical properties of various tropospheric aerosol types as determined from AERosol RObotic NETwork (AERONET) observations.

Due to the complexity of tropospheric aerosols, it is therefore useful to include in HITRAN refractive indices

that are based upon field experiments. Of particular interest to HITRAN 2012 are the indices of aerosols that contain absorptive characteristics, e.g. desert dust, minerals, burning vegetation, volcanic ash, carbonaceous flame, and brown carbon. Absorptive aerosol is characterized by a significant imaginary refractive index, and the influence of absorptive aerosol upon the Earth's atmosphere is the subject of current research [20]. Since aerosols evolve, e.g. becoming more likely to accept a coating of water over time, the optical properties also evolve. The papers associated with the tabulations of measured in-situ effective aerosol refractive indices contain textual information that describes the details of the measurements.

Table 1 lists the refractive indices included in HITRAN 2012. Indices of water, supercooled water, ice, binary liquid (H_2SO_4/H_2O, H_2SO_4/HNO_3), ternary liquid ($H_2SO_4/H_2O/HNO_3$), nitric acid dihydrate (NAD), nitric acid trihydrate (NAT), representative burning vegetation, and mineral compositions (e.g. sea salt, quartz, hematite), tabulated in HITRAN 2008 [12],

are part of HITRAN 2012. Additions to the previous listings include organic acids [39], secondary organic aerosol (proxy) [41], carbonaceous flame indices [36,37], mineralogical indices [42,43], volcanic ash indices [47], and biomass fire [35] and brown carbon [38] indices derived from field measurements. These materials are associated with tropospheric aerosols. We note that the measurements span limited ranges of wavelength between 0.25 and 50 μm. The HITRAN-RI program issues an error message when the requested calculation wavelength range falls outside of the range of the specified refractive index data file, states the data file's wavelength range, and requests the user to redefine the calculation's range of wavelength.

In regard to HITRAN 2012, refractive indices of aliphatic dicarboxylic acids (oxalic, malonic, succinic, and glutaric acid) and other acids (pyruvic, pinonic, benzoic, and phthalic) [39] at various weight percent compositions are tabulated for the real and imaginary indices from 0.25 to 1.25 μm and 0.25 to 1.1 μm, respectively. Dicarboxylic

Table 1
Refractive indices included in HITRAN 2012.

Compound	Measurement specifics	Reference
Water	27 °C, 10–5000 cm^{-1}	[21]
Water	0.67–2.5 μm	[22]
Ice	266 K, 0.04 μm–2 m	[23]
Ice	0.67–2.5 μm	[22]
Water, ice, sodium chloride, sea salt, water soluble aerosol, ammonium sulfate, carbonaceous aerosol, volcanic dust, sulfuric acid, meteoric dust, quartz, hematite, sand	Room temp, 0.2–40 μm	[16]
Sulfuric acid (H_2SO_4/H_2O)	Room temp, 25–96% H_2SO_4	[24]A
Sulfuric acid (H_2SO_4/H_2O)	Room temp, 75 and 90% H_2SO_4	[25]A
Sulfuric acid (H_2SO_4/H_2O)	215 K, 499–6996 cm^{-1}	[26]
Sulfuric acid (H_2SO_4/H_2O)	200–300 K, 825–4700 cm^{-1}	[27]
Sulfuric acid (H_2SO_4/H_2O)	213–293 K, 432–5028 cm^{-1}	[28]A
Nitric acid (H_2SO_4/HNO_3)	Room temp, 250–2987 cm^{-1}	[29]
Nitric acid (H_2SO_4/HNO_3)	220 K, 754–4700 cm^{-1}	[30]
Nitric acid (H_2SO_4/HNO_3)	213–293 K, 432–5028 cm^{-1}	[28]A
Amorphous nitric acid	153 K, 482–7000 cm^{-1}	[31]
NAM (nitric acid monohydrate)	179 K, 482–6002 cm^{-1}	[31]
NAD (nitric acid dihydrate)	184 K, 482–6981 cm^{-1}	[31]
NAD	160–190 K, 700–4700 cm^{-1}	[32]
αNAT (nitric acid trihydrate)	181 K, 482–6989 cm^{-1}	[31]
βNAT	196 K, 482–6364 cm^{-1}	[31]
NAT	160 K, 711–4004 cm^{-1}	[33]
Burning vegetation	525–5000 cm^{-1}	[34]
Burning vegetation	0.35–1.5 μm	[35]*
Carbon flame	0.4–0.7 μm, 25–600 °C	[36]*
Flame soot	0.2–38 μm	[37]*
Brown carbon	0.2–1.2 μm	[38]*
Organic acids Oxalic, malonic, succinic, pinonic, pyruvic, phthalic	0.25–1.1 μm	[39]*
Organic haze	0.525 nm	[40]*
SOA (proxy)	0.525 nm	[41]*
Minerals Clay, illite, kaolin, montmorillonite	2.5–200 μm	[42]*
Minerals Granite, montmorillonite	5–40 μm	[43]*
Saharan dust	0.30–0.95 μm	[44]*
Saharan dust	0.35–0.65 μm	[45]*
Saharan dust	0.35–0.65 μm	[46]*
Volcanic ash	0.45–25 μm	[47]*

Datasets in the 'archive' subdirectory are marked by an 'A'.
New HITRAN 2012 indices are marked by '*'.
Refractive indices included in HITRAN.

acids account for 1–15% of the total carbon aerosol, and occur in both the coarse and fine mode. Current research is focused upon understanding the role of organic chemistry in tropospheric aerosol processes. Since the imaginary refractive index of these acids is small, they have a scattering effect by themselves. Oxalic acid is the most abundant organic acid, and has the smallest molecular weight. It is thought that aqueous phase chemistry in fog and cloud droplets plays an important role in the formation chemistry of the organic acids and their products. The organic acids are also associated with isoprene chemistry that is associated with pine tree and other plant emissions.

Aqueous phase reactions of α-dicarbonyls (glyoxal and methylglyoxal) and amines (glycine and methylamine) produce droplets which, when dried, produce particles that have a brownish color [41]. The refractive indices of these particles have an imaginary index similar to HUmic-Like Substances (HULIS) measured in the field, and serve as a good model for secondary organic aerosol (SOA). The importance of these measurements is that models frequently assume that SOA has little visible light absorption. Since organic aerosol contributes 50% to the global aerosol mass in the troposphere, and 90% in urban regions [48], these absorption effects are potentially very important.

It is well known that desert dust is also absorptive. Desert dust and soil emissions are comprised of a variety of minerals, and the composition varies on a regional basis [49]. Indices from 2.5 to 50 μm of clay, illite, kaolin, and montmorillonite [42], granite and montmorillonite from 5 to 40 μm [43], and imaginary indices from 305 to 905 nm of African dust samples [44], add to the previous HITRAN mineral indices (quartz, hematite, and sand) [16]. The absorptive characteristics of desert dusts are dependent upon the hematite (iron) content of the dust. Hematite volume abundances from 1.1 to 2.7% of African dust samples yield a factor of two range in the imaginary indices. Fig. 1 presents the imaginary indices of the African dust samples [44], those derived from analysis of Total Ozone Mapping Spectrometer (TOMS) satellite and Aerosol Robotic Network (AERONET) data [45], and the Patterson et al. indices [46].

As illustrated by Fig. 1 of Ref. [17], and reviewed in Ref. [50], carbonaceous aerosol displays a wide variety of absorptive characteristics. Inclusion of these and other papers in the HITRAN-RI suite thereby informs the user of the variations of real world absorbing aerosols. The optical properties of brown carbon spheres in east Asian outflow over the Yellow Sea during the Asian Pacific Regional Aerosol Characterization (ACE-Asia) field program [38] are included in HITRAN 2012. Brown aerosols have imaginary indices somewhat smaller than black carbon particles. The imaginary index of the brown aerosol is greater than 0.2 between 0.2 and 1.2 μm, with larger values at the shorter wavelengths, indicating that scattering and absorption by brown carbon needs to be included in global models.

The 2010 eruptions of Eyjafjallajökull in Iceland halted aviation flights in Europe for 6 days, and dramatically emphasized the effects of volcanic eruptions upon commerce and the environment. Measurements of ash indices between 1 and 20 μm from samples gathered after the 1993 Mt. Aso eruption [47] are included in HITRAN 2012.

3. HITRAN-RI applications

HITRAN-RI is written in the Interactive Data Language (IDL) and Fortran 90 programming languages, with source code in separate subdirectories. The Aerosols_Readme.pdf file of the HITRAN-RI suite provides instructions on how to use the program. This file explains which program files need to be edited by the user, and also discusses the purposes and contents of the subdirectories. The IDL version conveniently exports the calculations to Postscript (PS) graphics files. Output ASCII files are written by the Fortran 90 program—the user then graphs the ASCII data using other software.

3.1. Refractive indices

HITRAN-RI can be used to compare two different sets of refractive indices. Fig. 2 displays the Tisdale [26] indices of refraction of H_2SO_4/H_2O at 75% H_2SO_4 and the Grainger [47] volcanic ash indices. Volcanic sulfate droplet extinction spectra are based upon H_2SO_4/H_2O indices, while larger ash particles contribute to the wavelength dependence soon after the volcanic eruption. Differences in the imaginary indices in the 8–10 μm range produce noticeable differences in the extinction spectra of the two materials, since the extinction spectrum in the infrared has a wavelength dependence that matches that of the imaginary index.

Since particles in the real world are frequently a mixture of compositions, mixing rules (average, Debye, Maxwell–Garnett, Bruggeman) are applied to estimate the aggregate indices of a multi-component particle. HITRAN-RI instructs the user on how to calculate the aggregate indices using the four mixing rules. Fig. 3 presents the aggregate refractive indices calculated using the four mixing rules for the case of quartz [16] with 0.05 (by volume abundance) hematite [16] inclusions. Differences
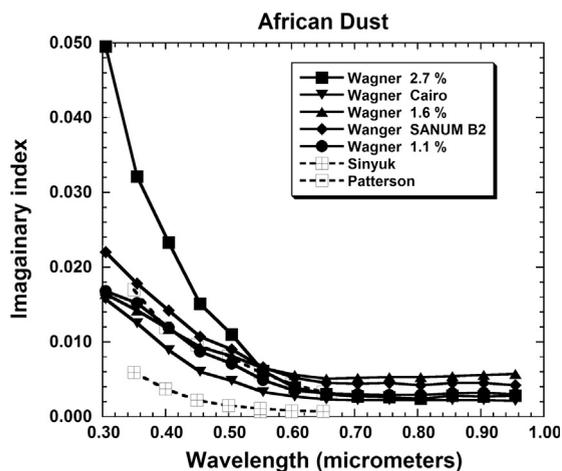

Fig. 1. Variations in the imaginary index of African dust [44–46]. The volume abundance of hematite is indicated for three of the Wagner [44] index sets.
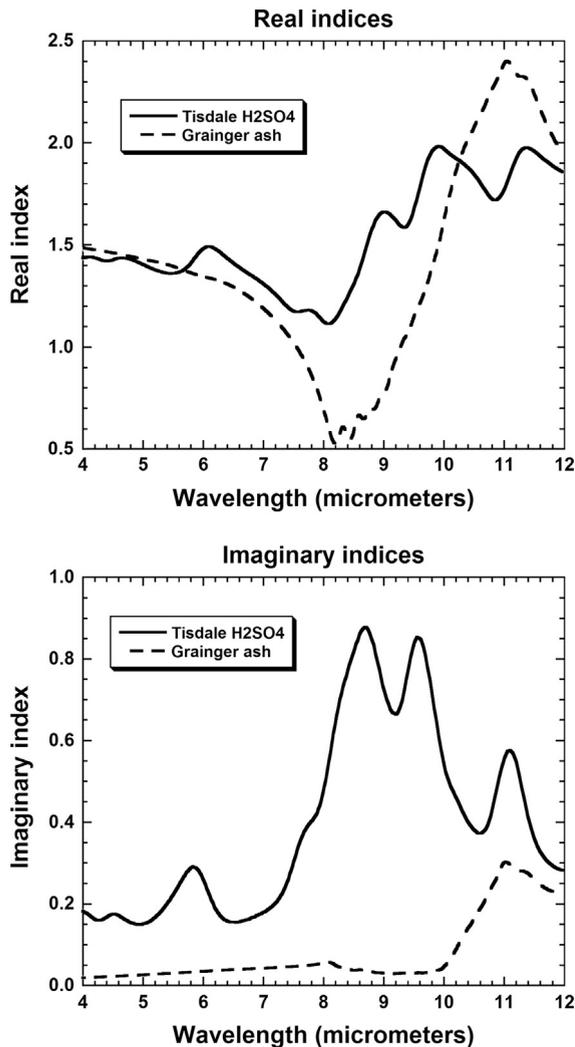
Fig. 2. Comparison of the Tisdale [26] indices of refraction of H_2SO_4/H_2O at 75% weight percent H_2SO_4 (i.e. stratospheric sulfate droplets) and the Grainger volcanic ash indices [47], calculated using HITRAN-HI.

Fig. 3. Refractive indices calculated using four different mixing rules for quartz [16] and 5% (by volume abundance) hematite [16] inclusions.

in the four sets of curves of the real and imaginary indices are apparent at both the peaks of the index structure and at various wavelengths between the peaks.

3.2. Calculation of specific optical properties

The standard application of HITRAN-RI is performed by specification of the size distribution, the index of refraction data set, and print flags in the "work.dat" ASCII input file. HITRAN-RI applies the "bhmie" Mie routine of Ref. [7]. Extinction, scattering, absorption, single scattering albedo, backscattering, and asymmetry spectra, the particle size distribution, and refractive index data are exported to output files, and postscript graphics files are generated by the IDL program. The output ASCII and netCDF data files can be used in external calculations. Since all lines of code are available to the user, the user can alter the format of the output files if desired.
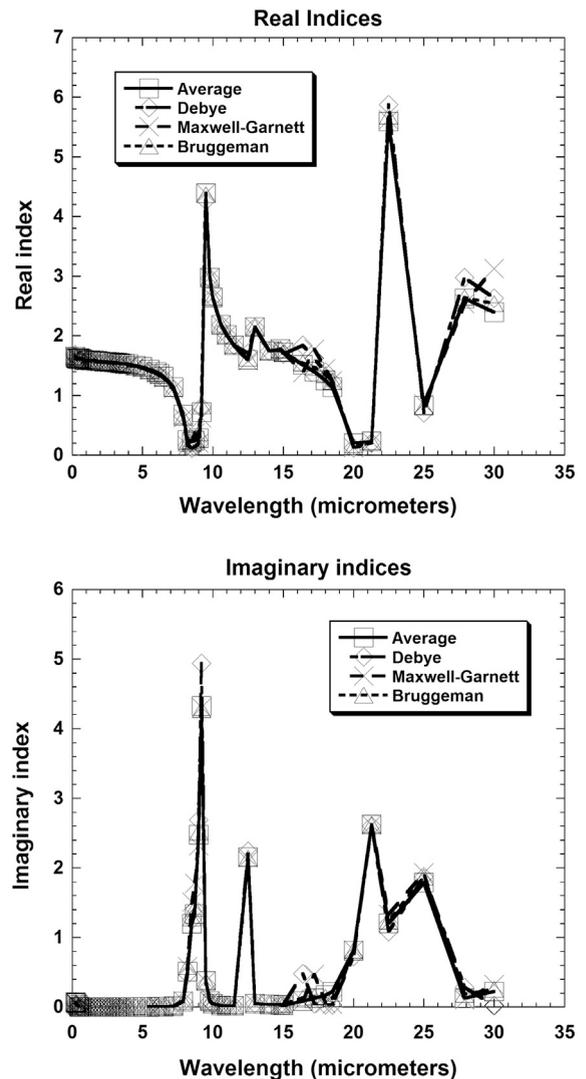
Given the same user specified size distribution and two different sets of indices, extinction spectra can be calculated in separate calculations to determine the range in extinction values that are due to differences (uncertainties) in the refractive indices. The pathnames of the output files of these two calculations can then be named in the "compare_spectra.dat" input ASCII file. Activation of a single flag in the "work.dat" input file then allows the user to compare the two calculations in numeric and graphic terms.

HITRAN-RI allows the user to specify input files that contain user specified indices of refraction and the size distribution for model calculation purposes. Specification of an observed extinction spectrum and the model calculation file pathnames in the "compare_spectra.dat" file then leads to a comparison of the two spectra. This feature is useful in exploratory calculations that seek to reconcile model and observed aerosol spectra.

3.3. Instructional/test cases

A number of test cases are instructional in regard to size distributions and Mie calculations. Input "work.dat" files and numerical and graphics test results are included in the "examples" and "output" subdirectories of the IDL code. These test cases serve as a convenient check on expected program performance.

The first test case illustrates representative size distributions, e.g. stratospheric sulfate before and after the Mt. Pinatubo volcanic eruption, a rain drop size distribution, the size distribution of Polar Stratospheric Cloud particles, a representative desert dust size distribution, and fine and coarse mode aerosol size distributions in clean rural and polluted urban settings. There are several ways to specify the size distribution (e.g. the number of particles per cm^3 per radii increment in μm, or number of particles per cm^3 per volume increment in μm^3). The first test case illustrates the various formulaic ways in which size distributions are specified for liquid and solid particles.

The Mie solution [6,7] specifies how light is absorbed and scattered by a sphere, with extinction being equal to the sum of scattering and absorption. The geometrical cross section πr^2 of a particle of radius r is effectively multiplied by an efficiency factor Q_{ext} (i.e. the sum of the Mie Q_{sca} and Q_{abs} terms). The second test case calculates Mie scattering Q_{sca} versus particle size parameter x (with $x=2\pi r/\lambda$, for particle radius r and wavelength λ) curves for a single particle, i.e. Fig. 5.7 of Ref. [1], followed by the calculation of corresponding Q_{ext} and Q_{abs} curves. Since Q_{ext} is a function of x and the complex refractive index $m=m_r+im_i$ where m_r and m_i are the real and imaginary refractive indices, this test case illustrates the dependence of Q_{ext} upon the imaginary index.

The third test case includes illustrative calculations in which the particle size distribution widens. Details of the single particle Q_{ext} versus x curve are smoothed by the extinction convolution integral of the extinction $\beta_{ext}(\lambda)$ spectrum

$$\beta_{ext}(\lambda) = 0.001 \int Q_{ext}(x,m)\pi r^2 dn/dr \, dr \qquad (1)$$

as the width of the size distribution dn/dr widens. The 0.001 factor in Eq. (1) is a units conversion factor, since $\beta_{ext}(\lambda)$ is usually expressed in km^{-1} units in remote sensing studies.

Tropospheric particles gain and lose surface coatings as the particles evolve. The effects of a surface coating are illustrated in the fourth test case by applying the "bhcoat" routine of Ref. [7]. For this application, the test case in Appendix B of Ref. [7] is applied. This test case shows the user how to calculate and compare graphically the optical properties of a particle with and without a user specified coating.

4. Discussion and future developments

HITRAN-RI will be updated on a continuing basis as more refractive index data are placed into the program. The goal of the first release is to establish the HITRAN-RI

framework, and provide to the user a way to use the HITRAN refractive indices in a convenient manner that readily connects the indices to atmospheric parameters (e. g. extinction, single scattering albedo).

The first release focuses upon the application of a Mie code, which is limited to spheres. Ice particles and "fractal" soot aggregrates, however, are very non-spherical. Public domain codes that perform non-spherical calculations using T-matrix and discrete dipole techniques are discussed in Refs. [51–54].

Refractive indices and papers to be added after the first release of HITRAN 2012 include the study of Hoffer et al. [55] of the optical properties of humic-like substances (HULIS) in biomass-burning aerosols, the work of Kirchstter et al. [56] on the spectral dependence of light absorption by aerosols affected by organic carbon, the discussion of Andrae and Gelencser [57] on black and brown carbon, the discussion of Bergstrom et al. [58] on the spectral absorption properties of atmospheric aerosols, and the extensive paper by Bond et al. [59] on the role of black carbon in the climate system. Updates to HITRAN are announced periodically on the HITRAN homepage.

Recent calculations [60–64] have produced a large database of ice crystal in-situ measurements, and optical properties of ice crystals of varying surface shapes (ice habits) and roughness. This extensive database is located outside of the HITRAN Harvard–Smithsonian website. HITRAN-RI will provide information to users on how to download this database, and will provide code by which a user can apply the data in ice crystal extinction spectrum calculations.

Acknowledgments

References

[1] Liou KN. An introduction to atmospheric radiation. San Diego: Academic Press; 2002.

[2] Thomas GE, Stamnes K. Radiative transfer in the atmosphere and ocean. Cambridge: Cambridge University Press; 1999.

[3] Rogers RR, Yau MK. A short course in cloud physics. Woburn: Butterworth Heinemann; 1989.

[4] Brasseur GP, Solomon S. Aeronomy of the middle atmosphere. Dordrecht: Springer; 2005.

[5] Seinfeld JH, Pandis SN. Atmospheric chemistry and physics. New York: John Wiley and Sons; 1998.

[6] van de Hulst HC. Light scattering by small particles. New York: Dover Publications; 1981.

[7] Bohren CF, Huffman DR. Absorption and scattering of light by small particles. New York: John Wiley and Sons; 1983.

[8] Crisp D, Boesch H, Brown L, Castano R, Christi M, Connor B, et al. OCO (Orbiting Carbon Observatory)—2 level 2 full physics retrieval algorithm theoretical basis, OCO D-65488, Version 1.0 Rev 4. Pasadena: Jet Propulsion Laboratory; November 10, 2010.

[9] Del Castillo C, Platnick S, Antoine D, Balch B, Behrenfeld M, Boss E, et al. Pre-Aerosol Clouds and ocean Ecosystem (PACE) mission science defintion team report. ⟨http://decadal.gsfc.nasa.gov/pace_documentation/PACE_SDT_Report_final.pdf⟩; 2012.

[10] Rothman LS, Gordon IE, Babikov Y, Barbe A, Benner DC, Bernath PF, et al. The HITRAN 2012 Molecular Spectroscopic Database. J Quant Spectrosc Radiat Transfer 2013. http://dx.doi.org/10.1016/j.jqsrt.2013.07.002, in press.

[11] Rothman LS, Jacquemart D, Barbe A, Benner DC, Birk M, Brown LR, et al. The HITRAN 2004 molecular spectroscopic database. J Quant Spectrosc Radiat Transfer 2005;96:139–204.

[12] Rothman LS, Gordon IE, Barbe A, Benner DC, Bernath PF, Birk M, et al. The HITRAN 2008 molecular spectroscopic database. J Quant Spectrosc Radiat Transfer 2009;110:533–72.

[13] Massie ST, Goldman A. The infrared absorption cross-section and refractive-index data in HITRAN. J Quant Spectrosc Radiat Transfer 2003;83:413–28.

[14] Husson N, Scott NA, Chédin A, Crépeau L, Armante R, Capelle V, et al. The GEISA spectroscopic database: current and future archive for Earth and Planetary atmosphere studies. J Quant Spectrosc Radiat Transfer 2008;109:1043–59.

[15] Hess H, Koepke P, Schult I. Optical properties of aerosols and clouds: the software package OPAC. Bull Am Meteorol Soc 1998;79:831–44.

[16] Fenn RW, Clough SA, Gallery WO, Good RE, Kneizys FX, Mill JD, et al. Optical and infrared properties of the atmosphere [Chapter 18]. In: Jursa AS, editor. Handbook of geophysics and the space environment. Springfield: National Technical Information Service; 1985.

[17] Twitty JT, Weinman JA. Radiative properties of carbonaceous aerosols. J Appl Meteorol 1971;10:725–31.

[18] Hinds WC. Aerosol technology—properties, behavior, and measurement of airborne particles. New York: Wiley-Interscience; 1999.

[19] Dubovik O, Holben B, Eck TF, Smirnov A, Kaufman YJ, King MD, et al. Variability of absorption and optical properties of key aerosol types observed in worldwide locations. J Atmos Sci 2002;59:590–608.

[20] Ramanathan V, Carmichael G. Global and regional climate changes due to black carbon. Natl Geogr 2008;1:221–7.

[21] Downing HD, Williams D. Optical constants of water in the infrared. J Geophys Res 1975;80:1656–61.

[22] Kou L, Labrie D, Chylek P. Refractive indices of water and ice in the 0.65–2.5 µm range. Appl Opt 1993;32:3531–40.

[23] Warren SG, Brandt RE. Optical constants of ice from the ultraviolet to the microwave: a revised compilation. J Geophys Res 2008;113: 1–10.

[24] Palmer KF, Williams D. Optical constants of sulfuric acid; application to the clouds of Venus? Appl Opt 1975;14:208–19.

[25] Remsberg EE, Lavery D, Crawford B. Optical constants for sulfuric and nitric acids. J Chem Eng Data 1974;19:263–5.

[26] Tisdale RT, Glandorf DL, Tolbert MA, Toon OB. Infrared optical constants of low-temperature H_2SO_4 solutions representative of stratospheric sulfate aerosols. J Geophys Res 1998;103:25353–70.

[27] Niedziela RF, Norman ML, Deforest CL, Miller RE, Worsnop DR. A temperature and composition-dependent study of H_2SO_4 aerosol optical constants using Fourier transform and tunable diode laser infrared spectroscopy. J Phys Chem A 1999;103:8030–40.

[28] Biermann UM, Luo BP, Peter T. Absorption spectra and optical constants of binary and ternary solutions of H_2SO_4, HNO_3, and H_2O in the mid infrared at atmospheric temperatures. J Phys Chem A 2000;104:783–93.

[29] Querry MR, Tyler IL. Reflectance and complex refractive indices in the infrared of aqueous solutions of nitric acid. J Chem Phys 1980;72:2495–9.

[30] Norman ML, Qian J, Miller RE, Worsnop DR. Infrared complex refractive indices of supercooled liquid HNO_3/H_2O aerosols. J Geophys Res 1999;104:30571–84.

[31] Toon OB, Tolbert MA, Koehler BG, Middlebrook AM, Jordan J. Infrared optical constants of H_2O ice, amorphous nitric acid solutions, and nitric acid hydrates. J Geophys Res 1994;99:25631–54.

[32] Niedziela RF, Miller RE, Worsnop DR. Temperature and frequency-dependent optical constants for nitric acid dihydrate from aerosol spectroscopy. J Phys Chem A 1998;102:6477–84.

[33] Richwine LJ, Clapp ML, Miller RE, Worsnop DR. Complex refractive indices in the infrared of nitric acid trihydrate aerosols. Geophys Res Lett 1995;22:2625–8.

[34] Sutherland RA, Khanna RK. Optical properties of organic-based aerosols produced by burning vegetation. Aerosol Sci Technol 1991;14:331–42.

[35] Magi BI, Fu Q, Redemann J. A methodology to retrieve self-consistent aerosol optical properties using common aircraft measurements. J Geophys Res 2007;112:D24S12. http://dx.doi.org/10.1029/2006JD008312.

[36] Stagg BJ, Charalampopoulos TT. Refractive indices of pyropytic graphite, amorphous carbon, and flame soot in the temperature range 25–600 °C. Combust Flame 1993;94:381–96.

[37] Chang H, Charalampopoulos TT. Determination of the wavelength dependence of refractive indices of flame soot. Proc R Soc Lond A 1990;430:577–91.

[38] Alexander DT, Crozier PA, Anderson JR. Brown carbon spheres in East Asian outflow and their optical properties. Science 2008;321: 833–6.

[39] Myhre CEL, Nielsen CJ. Optical properties in the UV and visible spectral region of organic acids relevant to tropospheric aerosols. Atmos Chem Phys 2004;4:1759–69.

[40] Hasenkopf CA, Beaver MR, Trainer MG, Dewitt HL, Freedman MA, Toon OB, et al. Optical properties of Titan and early earth haze laboratory analogs in the mid-visible. Icarus 2010;207:903–13.

[41] Zarzana KJ, De Haan DO, Freedman MA, Hasenkopf CA, Tolbert MA. Optical properties of the products of α-dicarbonyl and amine reactions in simulated cloud droplets. Environ Sci Technol 2012;46: 4845–51.

[42] Querry MR. Optical constants of minerals and other materials from the millimeter to the ultraviolet. Aberdeen: Chemical Research, Development Engineering Center, CRDEC-CR-88009; 1987.

[43] Toon OB, Pollack JB, Sagan C. Physical properties of the particles composing the martian dust storm of 1971–1972. Icarus 1977;30: 663–96.

[44] Wagner R, Ajtai T, Kandler K, Lieke K, Linke C, Müller T, et al. Complex refractive indices of Saharan dust samples at visible and near UV wavelengths: a laboratory study. Atmos Chem Phys 2012;12:2491–512.

[45] Sinyuk A, Torres O, Dubovik O. Combined use of satellite and surface observations to infer the imaginary part of refractive index of Saharan dust. Geophys Res Lett 2003;30:1081. http://dx.doi.org/10.1029/2002GL016189.

[46] Patterson EM, Gillette DA, Stockton BH. Complex index of refraction between 300 and 700 nm for Saharan aerosols. J Geophys Res 1977;82:3153–60.

[47] Grainger RG, Peters DM, Thomas GE, Smith AJA, Siddans R, Carboni E, et al. Measuring volcanic plume and ash properties from space. In: Pyle D, Mather T, editors. Remote sensing of volcanoes and volcanic processes: integrating observation and modeling. London: Special Publication Geological Society; 2013.

[48] Zhang Q, Jimenez JL, Canagaratna, Allan JD, Coe H, Ulbrich I, et al. Ubiquity and dominance of oxygenated species in organic aerosol in anthropogenically-influenced Northern Hemisphere mid-latitudes. Geophys Res Lett 2007;34:L13801.

[49] Nickovic S, Vukovic A, Vujadinovic M, Djurdjevic V, Pejanovic G. Technical note: high-resolution mineralogical database of dust-productive soils for atmospheric dust modeling. Atmos Chem Phys 2012;12:845–55.

[50] Bond TC, Bergstrom RW. Light absorption by carbonaceous particles: an investigative review. Aerosol Sci Technol 2006;40:27–67.

[51] Barber PW, Hill SC. Light scattering by particles, computational methods. New Jersey: World Scientific; 1990.

[52] Draine BT, Flatau PJ. Discrete-dipole approximation for scattering calculations. J Opt Soc Am 1994;A11:1491–9.

[53] Draine BT, Flatau PJ. User guide to the discrete dipole approximation code DDSCAT 7.2.2012. 〈http://arXiv.org/abs/1202.3424〉, 〈http://www.astro.princeton.edu/~draine/DDSCAT.html〉.

[54] Mishchenko MI, Travis LD, Mackowski DW. T-matrix computations of light scattering by nonspherical particles: a review. J Quant Spectrosc Radiat Transfer 1996;55:535–75.

[55] Hoffer A, Gelencsér A, Guyon P, Kiss G, Schmid O, Frank GP, et al. Optical properties of humic-like substances (HULIS) in biomass-burning aerosols. Atmos Chem Phys 2006;6:3563–70.

[56] Kirchstetter TW, Novakov T, Hobbs PV. Evidence that the spectral dependence of light absorption by aerosols is affected by organic carbon. J Geophys Res 2004;109. http://dx.doi.org/10.1029/2004JD004999.

[57] Andreae MO, Gelencser A. Black carbon or brown carbon? The nature of light-absorbing carbonaceous aerosols Atmos Chem Phys 2006;6:3131–48.

[58] Bergstrom RW, Pilewskie P, Russell PB, Redemann J, Bond TC, Quinn PK, et al. Spectral absorption properties of atmospheric aerosols. Atmos Chem Phys 2007;7:5937–43. http://dx.doi.org/10.5194/acp-7-5937-2007.

[59] Bond TC, Doherty SJ, Fahey DW, Forster PM, Berntsen T, DeAngelo BJ, et al. Bounding the role of black carbon in the climate system: a scientific assessment. J Geophys Res 2013;118:1–173.

[60] Cole B, Yang P, Baum BA, Redi J, C.-Labonnote L, Thieuleux F, et al. Comparison of PARASOL observations with polarized reflectances simulated using different ice habit mixtures. J Appl Meteorol Clim 2013;52:186–96.

[61] Yang P, Bi L, Baum BA, Liou KN, Kattawar GW, Mishchenko MI, et al. Spectrally consistent scattering, absorption, and polarization

properties of atmospheric ice crystals at wavelengths from 0.2 μm to 100 μm. J Atmos Sci 2012;70:330–47.

[62] Baum BA, Yang P, Heymsfield AJ, Schmitt CG, Xie Y, Bansmer A, et al. Improvements to shortwave bulk scattering and absorption models for the remote sensing of ice clouds. J Appl Meteorol Clim 2011;50: 1037–56.

[63] Baum BA, Yang P, Hu YX, Feng Q. The impact of ice particle roughness on the scattering phase matrix. J Quant Spectrosc Radiat Transfer 2010;111:2534–49. http://dx.doi.org/10.1016/j.jqsrt.2010.07.008.

[64] ⟨http://www.ssec.wisc.edu/ice_models/⟩.